Numerical modelling of sample–furnace thermal lag in dynamic mechanical analyser

Muhamed Sućeska · Zhi-Yue Liu ·
Sanja Matečić Mušanić · Ivona Fiamengo

Abstract Due to dynamic nature of processes taking place during the experiment (chemical reaction and physical processes, heat flow, gas flow, etc.) the results obtained by thermal methods may considerably depend on the conditions used during the experiment. Therefore, whenever the results of thermal analysis are reported, the experimental conditions used should be stated. In this paper we have studied the heat transfer from the furnace to the sample and through the sample during dynamic mechanical analysis measurements. Numerical modelling of the heat transfer was done using an own computer program based on the heat conduction equation, solved numerically applying the finite difference methods. The calculated values of the thermal lag between the furnace and the sample were compared with the values experimentally determined on samples of a composite polymeric energetic material (double-base rocket propellant). Also, the temperature distribution within sample as a function of the heating rate was analysed using the same numerical model. It was found out that using this model and temperature dependent heat transfer coefficient, experimentally obtained values of the thermal lag between the furnace and the sample can be satisfactory described. It was also shown that even at slow heating rates, such is, e.g. 2 °C min^{-1}, the thermal lag between the furnace and the sample can reach several degrees, while the thermal gradient within 3-mm thick rectangular sample can reach 0.4 °C.

Introduction

Thermal methods play an important role in analysis of different kinds of materials. However, many thermal methods are much less "compound specific" comparing to some other analytical techniques and the results obtained may considerably depend on the conditions used during the experiment [1]. The reasons for this are connected with dynamic nature of processes involved (extent and rate of reaction, extent and rate of change of property measured, transfer of the heat by conduction, convection and radiation around the apparatus, interaction of the surroundings with the sample, etc.). Therefore, whenever results of thermal analysis are reported, the conditions used should be included [1–4].

Dynamic mechanical analysis (DMA) is used to measure the modulus (stiffness) and damping (energy dissipation) properties of materials as they are deformed under periodic stress, at different temperature ranges. DMA is particularly useful for evaluating viscoelastic materials whose mechanical properties exhibit time, frequency and temperature effects [3].

In the DMA assembly, the sample is positioned in a temperature-controlled chamber which contains a radiation heater and a coolant distribution system. The coolant distribution system uses liquid nitrogen for controlled sub-ambient operation. An adjustable thermocouple, mounted close to the sample, provides precise feedback information to the temperature controller, as well as readout of furnace temperature (Fig. 1).

M. Sućeska (✉) · S. M. Mušanić · I. Fiamengo
Brodarski Institute – Marine Research & Special/Advanced Technologies, Av. V. Holjevca 20, 10020 Zagreb, Croatia
e-mail: suceska@hrbi.hr

Z.-Y. Liu
Beijing Institute of Technology, Zhongguancun South Avenue 5, 100081 Beijing, People's Republic of China
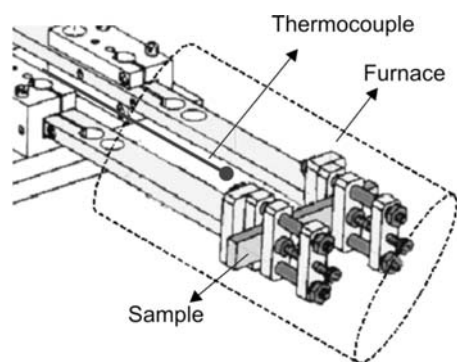
Fig. 1 Presentation of DMA apparatus (TA instruments, Model 983)

Like other thermal methods, DMA gives results that are dependent on the conditions used during the experiment; first of all on heating rate, sample dimension, surrounding atmosphere, frequency of deformation, etc. [1, 3, 5–8]. Among these factors the precise knowledge of the sample temperature during the measurements of physical properties of the sample has a major effect regarding the accuracy of the experiments.

There are two main reasons why it is not possible to attribute single temperature to the sample temperature—one is the existence of thermal gradient within the sample due to the sample's thermal resistance, and another is a thermal lag between different parts of the instrumentation set-up (between furnace and sample, between furnace and temperature sensor, etc.) [5–7]. The effect of the sample's own resistance in practice, especially if the sample is a bad heat conductor, is that there are different temperatures at different points of the sample (i.e. there is a temperature gradient within the sample); consequently true temperature of the sample in fact is an average sample temperature.

The heat transfer between the furnace and the different parts of the apparatus is not instantaneous, but will depend on the conduction, convection and radiation that can occur within the apparatus. There is bound to be a thermal lag between different parts of the apparatus, and the higher the rate of heating, the greater this lag is like to be.

The temperature sensor (thermocouple) in DMA apparatus is located very close to the sample, but it is separated from the sample by a thin gas gap. Due to this, there is a difference in the temperature of the furnace read by the sensor and the true temperature of the sample. To evaluate a true sample temperature, calibration procedures are well established for different thermal analysis techniques. General equation used to evaluate true sample temperature when working with different heating rates ($\beta = \mathrm{d}T/\mathrm{d}t$) is of the form [1, 6]:

$$T_\mathrm{F} = T_{\mathrm{S},0} + \tau \cdot \beta + a \tag{1}$$

where, T_F is the observed (by sensor) furnace temperature at heating rate β, $T_{\mathrm{S},0}$ is the true sample temperature, i.e.

temperature corresponding to $\beta = 0\ °\mathrm{C\ min^{-1}}$, τ is the so-called time-constant and a is the calibration constant.

The furnace temperature is read by the sensor and very often it is assumed to be equal to the sample surface temperature ($T_{\mathrm{S,s}}$). However, in the case of combined heat transfer from the furnace to the sample (by convection, conduction, and radiation) the sample surface temperature always differs from the furnace temperature and depends on the heat transfer from the furnace to the sample.

According to [6] the time-constant in Eq. 1 depends on the sample heat capacity (c) and two characteristic parameters of the apparatus—thermal resistance (R_0) and experimental constant τ_x:

$$\tau = \tau_x + R_0 c \tag{2}$$

In other words, in the case of constant heat capacity, the time-constant is directly related to the thermal resistance of a system ($R_0 \equiv \tau$).

A number of works has been devoted to study of the thermal lag between an apparatus furnace and the sample in thermal analysis apparatuses [5–11]. However, there are very few papers that numerically predict thermal parameters of thermal analysis techniques. If one is interested in understanding of the physical paths for heat transport, then numerical modelling of all heat transfer phenomena included is necessary.

In our previous paper [12] we have studied the influence of heating rate on results of DMA. We have shown that the reactive heat conduction equation [13] simplified to one-dimensional case and solved numerically applying the finite difference method [14] can be used to model the heat transfer phenomena in DMA apparatus. It was also shown [12] that the temperature dependent heat transfer coefficient should be used in order to reproduce experimentally obtained values of the thermal lag between furnace and sample. This is the consequence of the fact that the heat transfer coefficient depends on the sample and system geometry and size, property of fluid, temperature and other characteristics of the system in which heat transfer occurs [15–17].

In this paper we present the results of our continued study devoted to understanding of the experimental values of the thermal parameters of DMA equipment. In the paper we have modelled the heat transfer phenomena from the DMA furnace to the sample using the temperature dependent heat transfer coefficient.

Experimental

The experiments were carried out using a composite energetic material based on nitrocellulose as a matrix and diglycoldinitrate as a plasticizer (double-base rocket

propellant). The testing samples used in the study, being of rectangular shape (40 × 10 × 3 mm), were cut from the propellant grain.

All dynamic mechanical measurements were carried out on *TA Instruments* DMA, Model 983 in fixed frequency mode. The measuring conditions were:

– heating rate: 1, 2, 5 and 10 °C min^{-1}
– temperature range: −120 to +80 °C
– amplitude of deformation: ±0.2 mm
– frequency of an oscillatory load: 1 Hz

Description of numerical model applied

Simplified presentation of DMA furnace is given in Fig. 2. The heat transport from the furnace to the sample and other parts of the apparatus is mainly governed by conduction through the gas and by thermal radiation.

In the numerical model applied the following assumptions were made:

– furnace temperature changes in accordance with temperature program set by the user, and it is read by the temperature sensor located near the sample
– sample is of rectangular slab form, and length to thickness ratio of the sample is ∼10 (thus it may be considered as infinite slab and may be treated as one-dimensional case)
– effect of sample arms on the heat transport from the furnace to the sample is neglected
– there is no any measurable chemical reaction (e.g. decomposition of energetic compounds) in the temperature range applied (−120 to 80 °C)
– thermal conductivity and heat capacity are constant in the temperature range studied
– heat transfer coefficient changes with the furnace temperature.

The heat transfer equation in cylindrical co-ordinates has the following form [18, 19]:
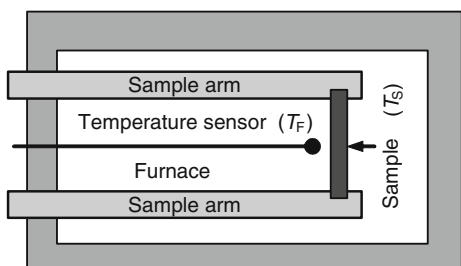
Fig. 2 Simplified presentation of DMA furnace–sample arrangement

$$\frac{\partial T}{\partial t} = \frac{\lambda}{c\rho}\left(\frac{\partial^2 T}{\partial r^2} + \frac{1}{r}\frac{\partial T}{\partial r} + \frac{\partial^2 T}{\partial z^2}\right) \tag{3}$$

where T is the temperature, t is the time, c is the specific heat capacity, ρ is the density, λ is the thermal conductivity, z is the axial position and r is the radial position.

In the special case of infinite slabs, long cylinders and sphere, Eq. 3 reduces in one dimension and may be expressed in the following form [20]:

$$\frac{\partial T}{\partial t} = \frac{\lambda}{c\rho}\left(\frac{\partial^2 T}{\partial r^2} + \frac{m}{r}\frac{\partial T}{\partial r}\right) \tag{4}$$

The integer m has the value 0 for slabs, 1 for cylinders and 2 for sphere. In the case of an infinite slab, r is replaced by the slab thickness (x).

The time dependent solution of Eq. 4 can be obtained by applying the finite difference method, i.e. by approximating partial derivatives with finite differences.

The time derivative in Eq. 4 may be replaced by its simplest finite difference approximation [14]:

$$\left(\frac{\partial T}{\partial t}\right) = \frac{T_i^{j+1} - T_i^j}{\Delta t}, \tag{5}$$

where Δt is a time increment.

For the case of an infinite slab the space derivatives in Eq. 4, in time j, may be approximated by the following finite differences [14, 21]:

$$\left(\frac{\partial^2 T}{\partial x^2}\right) = \left(\frac{T_{i+1}^j + T_{i-1}^j - 2T_i^j}{(\Delta x^2)}\right) \tag{6}$$

By replacing the space and time derivatives in Eq. 4 by the finite differences (Eqs. 5, 6), the equation for the calculation of the temperature distribution along a space co-ordinate, at time t^{j+1} can be derived. In the case of an infinite slab, this equation will be:

$$T_i^{j+1} = T_i^j + \frac{\lambda(\Delta t)}{c\rho}\left(\frac{T_{i+1}^j + T_{i-1}^j - 2T_i^j}{(\Delta x^2)}\right) \tag{7}$$

It follows from the above equation that the temperature distribution along the slab thickness at time t^{j+1} is evaluated from the temperature distribution at earlier time (t^j), where:

$$t^{j+1} = t^j + \Delta t \tag{8}$$

In addition to the finite difference approximation to the reactive heat conduction equation, the approximations to the initial and boundary conditions should be included in order to calculate the time–temperature distribution along the specimen space co-ordinate. The initial conditions give an initial temperature distribution (at $t = 0$) along the specimen co-ordinate. In the most usual way the initial conditions are given in the form:

$$T_i^{j=0} = T_{0,i}^{j=0}, \quad \text{where } i = 0, 1, 2, 3 \ldots k - 1 \quad (9)$$

The boundary conditions give the temperature at the specimen surface at any time ($T_{S,s}^j$). The simplest case is when the specimen surface temperature equals the furnace temperature during the whole process. However, in the case of a combined heat transfer from the furnace to the specimen surface (by radiation and convection), the boundary conditions are given by the following equation [14, 21, 22]:

$$\varepsilon(T_{S,s} - T_F) = -\lambda \frac{T_{S,s} - T_{k-1}}{\Delta r} \quad (10)$$

where ε is the overall heat transfer coefficient (Wm^{-2} K^{-1}), T_F is the furnace temperature and T_{k-1} is sample temperature in the layer adjacent to the sample surface [14].

As mentioned before, the heat transfer coefficient depends on many factors, such as geometry of the sample and the system, property of fluid, temperature and other characteristics of the system in which heat transfer occurs. The variation of the heat transfer coefficient with temperature has been subject of many investigations, however, no universal behaviour was found since the effect of temperature on the surface heat transfer coefficient depends on the actual experimental conditions.

It was found [16–18] that the heat transfer coefficient is strong non-linear function of temperature. Chang [17] has described dependence of the heat transfer coefficient on temperature difference between the sample surface ($T_{S,s}$) and the surrounding fluid temperature applying a power-law type of equation:

$$\varepsilon = b(T_{S,s} - T_F)^n \quad (11)$$

where b is dimensional constant defined by physical properties of the surrounding medium and n is exponent dependent on heat transfer mechanism.

The following type of equation, based on the fact that the heat transfer coefficient is inversely proportional to the thermal resistance, may be also used to describe its dependences on temperature [18]:

$$R = R_{ref}\left(\frac{T}{T_{ref}}\right)^n, \quad \text{i.e. } \varepsilon = \varepsilon_{ref}\left(\frac{T_{ref}}{T}\right)^n \quad (12)$$

where subscript 'ref' refers to a reference temperature.

Results and discussion

To study experimentally the thermal lag between the furnace and the sample in the DMA apparatus we have used double-base propellant based on nitrocellulose and diglycoldinitrate. This material exhibits viscoelastic behaviour.
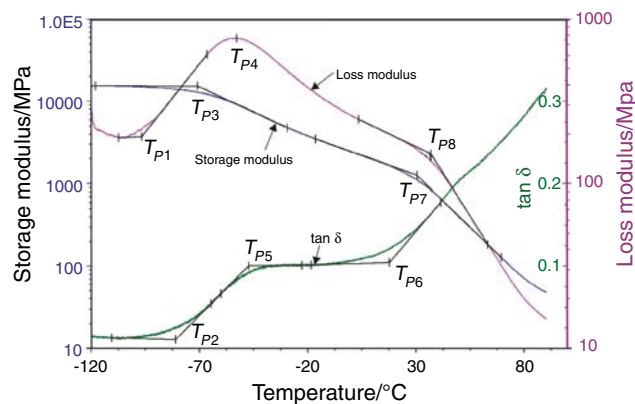

Fig. 3 Storage modulus, loss modulus and tan δ curves for tested double-base rocket propellant (at $\beta = 2$ °C min^{-1})

The DMA curves obtained (Fig. 3) are typical for such kind of materials: the storage modulus (E') is almost constant until about −70 °C, when a slow drop takes place with temperature as a consequence of the glass transition. Another distinct change in the storage modulus slope is visible at about 30 °C, corresponding to the sample softening. The maximum of the loss modulus (E'') at about −56 °C corresponds to the glass transition temperature. The tan δ also increases at the glass transition region, as well as at the softening region.

Eight characteristic points, corresponding to transition from the glassy to the viscoelastic and from the viscoelastic to the softening region were identified on DMA curves (Fig. 3), and the temperatures at these points were used to study experimentally thermal lag between the sample and the furnace. The onset temperatures at these points, assigned as T_{P1}–T_{P8}, correspond to the beginning of certain process/transition in the sample. For the sake of simplicity these temperatures in the paper will be called transition temperatures. The physical meaning and denotation of individual characteristic temperatures are given in Table 1.

Experimental determination of thermal lag

To test the influence of heating rate on the thermal lag, the samples were subjected to DMA experiments at different heating rates: 1, 2, 5 and 10 °C min^{-1}. As the heating rate increases, the temperatures of transitions (T_{P1}–T_{P8}) increase. As mentioned earlier, such behaviour is the consequence of an increase of the thermal lag between the sample and the furnace, as well as the thermal gradient within the sample with heating rate increase. Typical shift of DMA curves with heating rate is illustrated in Fig. 4.

It is well-known that a certain transition in the sample begins after the sample has reached a temperature at which this transition starts ($T_{transition}$), and consequently the sample temperature (T_S) is equal to the transition temperature

Table 1 Characteristic temperatures on DMA curves used to study thermal lag dependence on heating rate

Temperature of transition	Description and physical meaning	Temperature of a given transition (at $\beta \rightarrow 0$ °C min^{-1})/°C
T_{P1}	The first onset on E''–T curve (beginning of glass transition region)	−97.22
T_{P2}	The first onset on tan δ–T curve (beginning of glass transition region)	−83.55
T_{P3}	The first onset on E'–T curve (beginning of glass transition region)	−71.47
T_{P4}	Maximum on E''–T curve (glass transition temperature)	−56.23
T_{P5}	The second onset/maximum on tan δ–T curve (glass transition temperature)	−50.21
T_{P6}	The third onset on tan δ''–T curve (beginning of softening)	−13.81
T_{P7}	The second onset on E'–T curve (beginning of softening)	26.21
T_{P8}	The second onset on E''–T curve (beginning of softening region)	32.31

($T_S = T_{\text{transition}}$.). This is principle upon which the calibration of thermal methods apparatus is based. According to Eq. 1 at the zero value of heating rate, the thermal lag equals zero, and thus the furnace temperature will be equal to the sample temperature ($T_F = T_{S,0}$), i.e. to the transition temperature ($T_F = T_{\text{transition}}$.). For example, the temperature assigned as T_{P4} on the E''–T curve (Fig. 4) corresponds to the glass transition (T_g). The glass transition temperature extrapolated to zero heating rate is true glass transition temperature ($T_{g,0}$) of a given sample. The dependence of the transition temperatures on heating rate is given in Fig. 5.

Dependence of the transition temperatures on heating rate is linear. However, the slopes of curves increase with the transition temperatures increase. This means that the time-constant increases with the heating rate increase (Eq. 1). This is clearer from Fig. 6 showing dependence of the thermal lag ($T_F - T_{S,0}$) on the heating rate.

It is obvious from Figs. 5 and 6 that for the same heating rate the thermal lag increases with the sample transition temperature, and the slope of ($T_F - T_{S,0}$)–β curves increases with the transition temperature as well. The increase of thermal lag with temperature is connected primarily with the change of thermal resistance of the system, and with the increase of temperature gradient
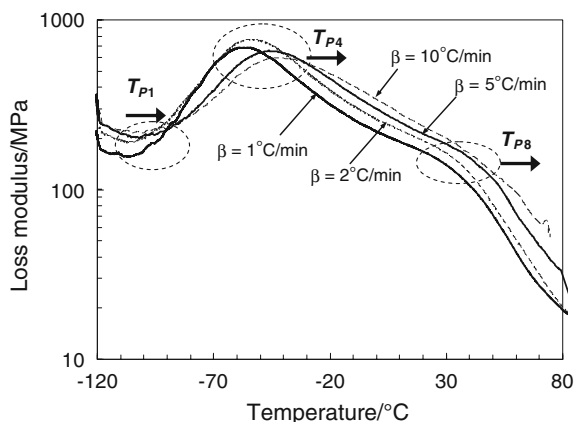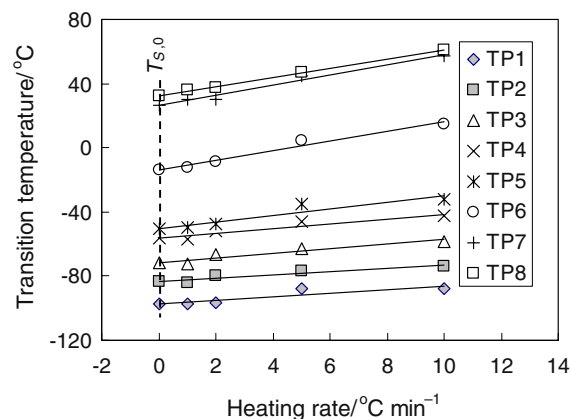

Fig. 5 Dependence of sample transition temperatures on heating rate
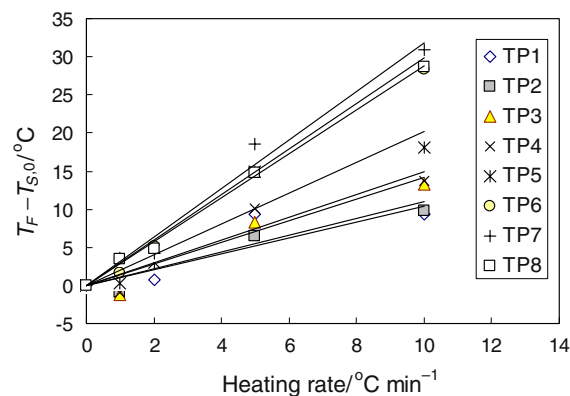

Fig. 6 Thermal lag at individual sample transition temperatures versus heating rate

within the sample with the heating rate. Figure 6 also shows that the thermal lag is considerable even at slow heating rates (e.g. up to 5 °C at $\beta = 2$ °C min^{-1}). At higher heating rates it can reach more than dozens of degrees (e.g. up to 30 °C at $\beta = 10$ °C min^{-1}).

As follows from Eq. 1, the thermal lag dependence on the heating rate may be expressed as:

$$(T_F - T_{S,0}) = \tau \cdot \beta + a \tag{13}$$

Fig. 4 Loss modulus versus temperature at different heating rates

By the linear regression analysis of the experimentally obtained dependence of thermal lag on heating rate (Fig. 6), the time-constants at individual transition temperatures and the constant a are determined. The mean value of constant a equals 0.00053 °C, while the time-constant increases with the transition temperature increase (Fig. 7).

Since the time-constant is directly related to the thermal resistance (Eq. 2), the data given in Fig. 7 clearly show that the thermal resistance of the system increases with temperature.

Alves et al. [5] have found for Perkin Elmer DMA7e apparatus similar behaviour—almost linear increase of the transition temperature (melting of indium) with the heating rate in the compression and tree-points bending modes, however, in the extension mode they observed a decrease of the transition temperature with the heating rate. Such unexpected behaviour the authors explain by the combination of the complex flow of the purge gas with the irradiation of heat from the furnace wall.

Roura and Farjas [6] have studied temperature dependence of the time-constant in a differential thermal analyser (DTA), in argon atmosphere and in temperature range 200–1,500 °C. They have found that the time-constant decreases nonlinearly with temperature. This is opposite to our findings, but it should be mentioned that their findings cannot be directly compared with our results (since we used different thermal techniques having different geometry, different temperature range and probably different heat transfer mechanism, etc.). These examples illustrate the complexity of temperature dependence of thermal resistance in thermal methods apparatuses.

Calculation of thermal lag between furnace and sample

On the basis of the model described an own computer program was developed. The program enables modelling of the heat transfer from the furnace to the sample, as well as
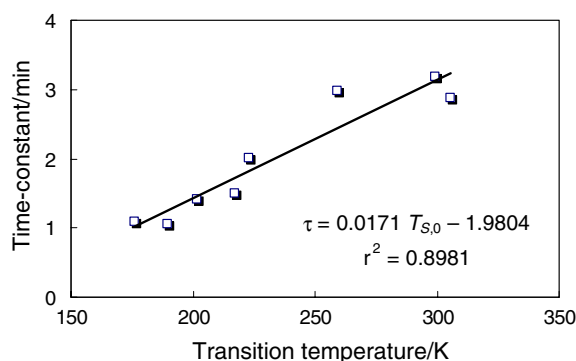

Fig. 7 Dependence of time-constant on temperature

the heat transfer within the sample during the entire experiment. The following values of parameters in the heat conduction equation (Eq. 7) are used in the calculation:

- sample density (ρ_0): 1.6 g cm^3
- sample thermal conductivity (λ): 0.16 W m^{-1} K^{-1}
- sample specific heat capacity (c): 1.254 J g^{-1} K^{-1}
- boundary conditions: heat transfer from the furnace to the sample by radiation and convection (Eq. 11)
- heat transfer coefficient (ε): dependent on temperature

Values of the heat transfer coefficient as a function of temperature are derived applying two methods:

Method 1: Values of the heat transfer coefficient are adjusted (by successive trials) to give the best agreement between experimentally obtained and calculated thermal lag for a given sample transition temperature. In other words, a constant value of the heat transfer coefficient is modified until the best agreement for one transition temperature is obtained, than another constant value is adjusted to obtain the heat transfer coefficient for another transition temperature, etc. In this way for each sample transition temperature the corresponding heat transfer coefficients are determined.

Method 2: The method is based on the fact that in the case of constant heat capacity the time-constant is proportional to the thermal resistance ($R_0 \equiv \tau$, Eq. 2), and the fact that the heat transfer coefficient is inversely proportional to the thermal resistance ($\varepsilon \equiv 1/R_0$). From these two relations it follows:

$$\varepsilon = k_\mathrm{p}\frac{1}{\tau} \tag{14}$$

where k_p is proportionality and unit conversion constant.

In this model the time-constant changes continuously with the furnace temperature according to the equation derived by linear regression analysis of experimentally obtained τ–T dependency given in Fig. 7:

$$\tau = 0.0171T - 1.9804$$
$$\text{(where } T \text{ is expressed in } K, \tau \text{ in minutes)} \tag{15}$$

Values of the heat transfer coefficient at a given furnace temperature are determine by adjusting the proportionality constant (by successive trial) to give the best overall agreement between the experimentally obtained and calculated thermal lag for all sample transitions temperatures. It was found that $k_\mathrm{p} = 44.2$ W min m^{-2} K^{-1} gives the best overall agreement.

Values of the heat transfer coefficient as a function of the furnace temperature, obtained in this way, are presented in Fig. 8.

Figure 8 shows that in the temperature range studied (−100 to 35 °C) the heat transfer coefficient decreases non-linearly with the furnace temperature. It was found out

by non-linear regression analysis of all data points, i.e. the data points obtained by two different methods, that both methods can satisfactory describe obtained ε–T dependence:

$$\varepsilon = k_p \frac{1}{\tau} = 44.2 \left(\frac{1}{0.0171T - 1.9804} \right), \quad r^2 = 0.9942 \tag{16}$$

$$\varepsilon = \varepsilon_{ref} \left(\frac{T_{ref}}{T} \right)^n = 14.36 \left(\frac{298.15}{T} \right)^{1.9786}, \quad r^2 = 0.9886 \tag{17}$$

The temperature in Eqs. 16 and 17 is expressed in K, the reference temperature (T_{ref}) is taken to be 298.15 K, the heat transfer coefficient at reference temperature (ε_{ref}) was found to be 14.36 W m^{-2} K^{-1} and the proportionality constant (k_p) equals 44.2 W min m^{-2} K^{-1}.

It is not easy to explain in a simple way experimentally obtained behaviour of the heat transfer coefficient because it depends on a number of parameters (e.g. geometry of the system and sample, fluid type and properties, temperature, velocity of fluid, heat transfer mechanism, heat fluxes resulting from the existence of hot and cold parts and other characteristics of the system in which heat transfer occurs). This is the reason why it is necessary to derive experimentally the value of the heat transfer coefficient for each system, and why it is not possible to compare directly the results obtained for different systems.

Based only on the fact that the heat conductivity of nitrogen, as a fluid that conducts the heat in DMA experiments, increases with temperature, one could expect an increase of the heat transfer coefficient with temperature too. However, the results obtained indicate that the behaviour of the heat transfer coefficient is much more complex and should be connected with all parameters that can influence the heat transfer behaviour. The complexity of the heat transfer behaviour in DMA experiments may be illustrated by the following example: increase of temperature causes increase of the thermal conductance of nitrogen and increase
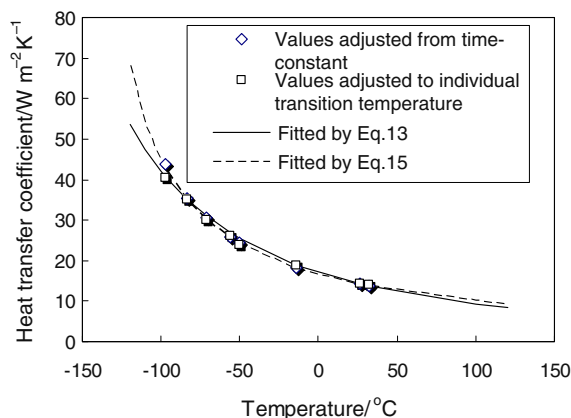
of the heat transfer coefficient, but at the same time increase of temperature causes increase of viscosity of nitrogen, which decreases its value, etc.

Comparison of experimental and calculated results

Verification of the calculation results was done by comparing the experimental and the calculated values of thermal lag for all transition temperatures and for all heating rates. The results of comparison, obtained using dependence of the heat transfer coefficient on furnace temperature given by Eq. 16, are given in Figs. 9 and 10.

Figure 9 shows that there is good agreement between the calculated and experimentally obtained transition temperatures at different heating rates, while Fig. 10 shows satisfactory agreement for the thermal lag at different heating rates versus sample temperatures. This confirms that the temperature dependent heat transfer coefficient can satisfactorily reproduce experimentally obtained heat transfer from the DMA apparatus furnace to the sample.
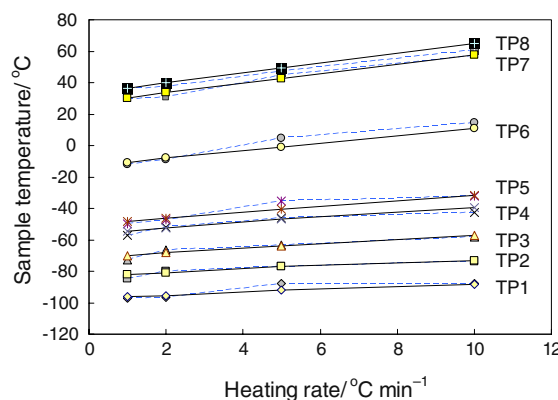
Fig. 9 Comparison of experimental and calculated values of sample transition temperatures versus heating rates (*solid line*—calculation result, *dashed lines*—experimental data)
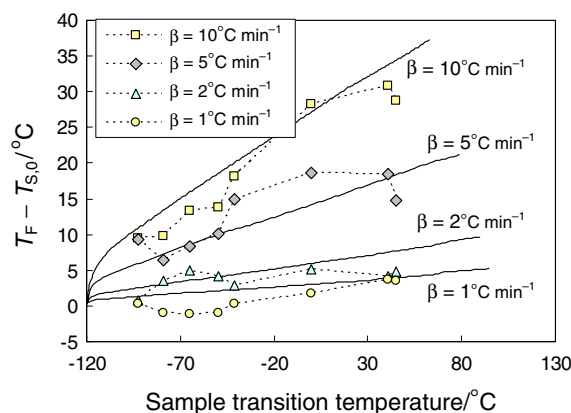
Fig. 8 Dependence of heat transfer coefficient on furnace temperature

Fig. 10 Dependence of thermal lag at different heating rates on sample transition temperature (*solid line*—calculation result, *dashed lines*—experimental data)
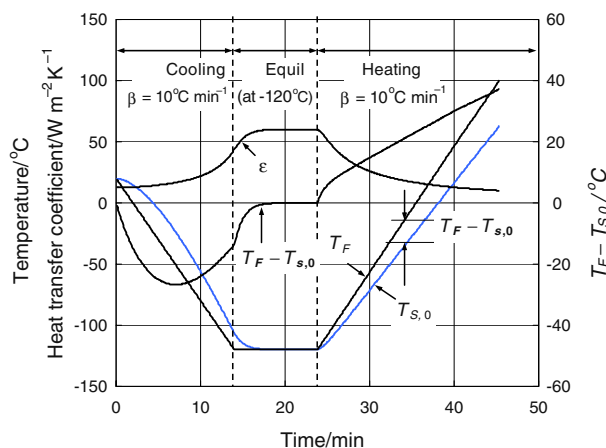
Fig. 11 Calculated furnace temperature, sample temperature, thermal lag and heat transfer coefficient versus time during DMA experiment

Fig. 12 Calculated temperature gradient-thickness profiles at different times (i.e. sample surface temperature) at 10 °C min^{-1} heating rate

The calculation results for a typical DMA experiment which includes the cooling of the sample from the room temperature to specified sub-ambient temperature, then equilibration, and then heating to desired final temperature are presented in Fig. 11.

The experiment starts at 20 °C (at that point the furnace and the sample are at the same temperature of 20 °C), and then the furnace is cooled down up to −120 °C with 10 °C min^{-1} cooling rate. Due to the thermal lag, the sample temperature at the beginning of the cooling period is higher than the furnace temperature. The difference between these two temperatures increases up 26 °C, and then starts to decrease due to power-law increase of the heat transfer coefficient with decrease of temperature. At the end of the cooling period the difference between the furnace and the sample temperatures equals 13 °C. To attain the same temperature of the furnace and the sample before the heating stage, and to attain the same temperature through the sample, an isothermal equilibration period is allowed at −120 °C. The calculation has shown that minimum period of 5 min is necessary for such equilibration. At the heating stage the temperature of the furnace is higher than the sample temperature, and due to the fact that the heat transfer coefficient decreases with temperature this, difference (i.e. thermal lag) increases during the experiment.

Calculation of time and space distribution
of temperature through sample

Due to an own resistance of the sample there is always a temperature gradient, i.e. different temperatures at different points of the sample, during DMA experiments. The temperature gradient depends on the sample dimensions and shape, thermal conductivity of the sample and heating rate.

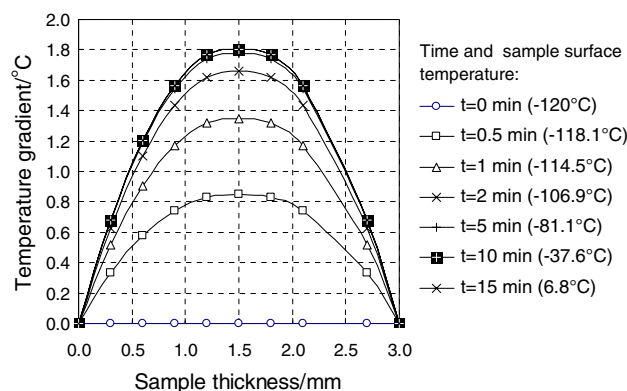As an example the calculated temperature gradients at different times versus sample thickness profile are given in Fig. 12. In the calculation the sample thickness was divided into 20 cells the thickness of which was 0.15 mm. The temperature at the sample surface was specified by the boundary conditions given by Eq. 10.

At the beginning of the experiment temperature is uniform through the sample and it equals −120 °C. When heating starts, the sample surface temperature increases, while the sample central temperature remains lower due to the thermal resistance of the sample. At 10 °C min^{-1} heating rate the difference between the sample surface and central temperatures reaches about 1.8 °C after about 10 min. For slower heating rates the temperature gradient is lower, but it is still significant. For example, at $\beta = 1$ °C min^{-1} the temperature gradient equals to about 0.2 °C.

In other words, the sample surface temperature read by the sensor and the true sample temperatures are different. This difference, as well as the thermal lag, increases with the heating rate increase, and the result is a shift of DMA curves to higher temperatures by the heating rate increase.

Conclusions

The results presented in the paper have shown that there is a considerable thermal lag between the furnace and the sample, as well as a significant temperature gradient through the sample during DMA experiments. Both the thermal lag and the temperature gradient increase with the heating rate applied during the measurement and with the furnace temperature.

The results have confirmed that by the numerical model described, and by varying the heat transfer coefficients as a power-law function of furnace temperature, the experimentally obtained thermal lag between the furnace and the sample can be reproduced in a satisfactory way. As such, the

model can be used to analyse and to model the heat transfer phenomena, and can give a qualitative and quantitative insight how the thermal lag and the temperature gradient in the sample can affect the results of measurement. This information is necessary if one wants to understand physical paths of the heat transfer in a DMA apparatus, as well as to understand correctly the results obtained. Also, the model can help in choosing such experimental conditions that will minimise possible effects of the thermal lag on the results.

It was determined experimentally that at the heating rate of 10 °C min^{-1} the thermal lag may reach more than 10–30 °C (depending on the furnace temperature), while the temperature gradient at the same heating rate reaches 1.8 °C. At slower heating rates both the thermal lag and temperature gradient decrease, but they are still significant even at 1–2 °C min^{-1} heating rates.

It was found that in the temperature range between −100 and 35 °C, the heat transfer coefficient decreases non-linearly with the furnace temperature. In the temperature range studied experimentally, the heat transfer coefficient decreases from 45 W m^{-2} K^{-1} at −97 °C to 13.5 W m^{-2} K^{-1} at 32 °C. Such non-linear behaviour of the heat transfer coefficient means that it is very sensitive to small changes of the furnace temperature, particularly at lower temperatures (below −50 °C).

The analysis of temperature dependence of the heat transfer coefficient has shown that it can be satisfactorily described by two types of equations: reciprocal model based on inverse proportionality between the heat transfer coefficient and the time-constant, and by the power-law model. However, it should be noted that the dependence obtained by the regression analysis is reliable for the temperature range −100 °C and 35 °C, for which experimental data for the thermal lag were determined.

The temperature dependence of thermal lag implicates that the temperature calibration of DMA apparatus should be done using more than one standard material in order to obtain reliable results in a broader temperature range, i.e. in the range of interest.

References

1. Hines PJ. Thermal methods of analysis-principles: applications and problems. London: Bleckie Academic & Professional; 1992. p. 139–54.

2. Quantitative Calculations and Theoretical Principles of the 983 Dynamic Mechanical Analyzer. TA Instruments. TA-032.

3. Murayama T. Dynamic mechanical analysis of polymeric materials. Amsterdam: Elsevier Scientific Publishing Company; 1978. p. 19–22.

4. Ozawa T. Thermal analysis—review and prospects. Thermochim Acta. 2000;355:35–42.

5. Alves NM, Mano JF, Gomez Ribbels JL. Analysis of the thermal environment inside the furnace of a dynamic mechanical analyser. Polym Test. 2003;22:471–81.

6. Roura P, Farjas J. Analysis of the sensitivity and sample–furnace thermal lag of a differential thermal analyser. Thermochim Acta. 2005;439:115–22.

7. Lacik I, Krupa I, Stach M, Kučma A, Jurčiova J, Chodak I. Thermal lag and its practical consequence in the dynamic mechanical analysis of polymers. Polym Test. 2000;19:755–71.

8. Mano JF, Cahon JP. A simple method for calibrating the temperature in dynamic mechanical analysers and thermal mechanical analysers. Polym Test. 2004;23:423–30.

9. Van Ekeren PJ, Bevers RT. Temperature calibration of a high-pressure DSC for measurements in ammonia. J Therm Anal Calorim. 2007;90:931–4.

10. Alouani K, Siniti M, Claudy P. Heat transfer in a DSC-type DSC apparatus. J Therm Anal Calorim. 2007;89:37–43.

11. Yazdi MH, Lee-Sullivan P. Determination of dual glass transition temperatures of a PC/ABS blend using two TMA modes. J Therm Anal Calorim. 2009;96:7–14.

12. Sućeska M, Liu ZY, Matečić Mušanić S. Numerical modelling of effect of heating rate on results of dynamic mechanical analysis of rocket propellants. Proceedings of the 10th Seminar "New trends in research of Energetic Materials". Pardubice. Czech Republic; 2007. pp 904–917.

13. Merzhanov AG, Abramov VG. Thermal explosion of explosives and propellants. A review. Propellants Explos. 1981;6:130–48.

14. Sućeska M. A computer program based on finite difference method for studying thermal initiation of explosives. J Therm Anal Calorim. 2002;68:865–87.

15. Aguilar G, Verkruysse W, Majaron B, Svaasand LO, Lavernia EJ, Nelson JS. Measurement oh heat flux and heat transfer coefficient during continuous cryogen spray cooling for laser dermatologic surgery. IEE J Select Top Quant Electron. 2001;7(6):1013–21.

16. Chang MH. A decomposition solution for fins with temperature dependent surface heat flux. Int J Heat Mass Transf. 2005;48:1819–24.

17. Cheng H, Xie J, Li J. Determination of surface heat-transfer coefficients of steel cylinder with phase transformation during gas quenching with high pressures. Comput Mater Sci. 2004;29:453–8.

18. Paasschens JCJ, Harmsa S, van der Toorn R. Dependence of thermal resistance on ambient and actual temperature. Proceedings of the 2004 Bipolar/BiCMOS Circuits and Technology Meetings. Montréal. Canada; 2004. pp 96–99.

19. Buehler FU, Seferis JC. Heat diffusion analysis of the temperature distribution and phase lag build-up in TMDSC specimens. Thermochim Acta. 1999;334:49–55.

20. Mader CL. Numerical modeling of explosives and propellants. Boca Raton: CRC Press; 1998. p. 136–87.

21. Anderson CA. TEPLO—a heat conduction code for studying thermal explosion in laminar composites. Report LA-4511. Los Alamos Scientific Laboratory. Los Alamos; 1970.

22. Isler J, Kayser D. Correlation between kinetic properties and self-ignition of nitrocellulose. Proc. of 6th Symp. Chem. Probl. Connected Stab. Explos. Kungalav. Sweden; 1982. pp. 217–237.